AGU PUBLICATIONS

Geophysical Research Letters

RESEARCH LETTER
10.1002/2015GL066850

Key Points:
- MESSENGER regularly detected suprathermal (<10 keV) electrons from orbit about Mercury
- The majority of these electrons were clustered near Mercury's magnetic equator
- Accelerated electrons are injected from Mercury's tail to form a quasi-trapped population

Correspondence to:
G. C. Ho,
george.ho@jhuapl.edu

Citation:
Ho, G. C., et al. (2016), MESSENGER observations of suprathermal electrons in Mercury's magnetosphere, *Geophys. Res. Lett.*, *43*, 550–555, doi:10.1002/2015GL066850.

Received 2 NOV 2015
Accepted 11 DEC 2015
Accepted article online 17 DEC 2015
Published online 23 JAN 2016

MESSENGER observations of suprathermal electrons in Mercury's magnetosphere

George C. Ho[1], Richard D. Starr[2], Stamatios M. Krimigis[1,3], Jon D. Vandegriff[1], Daniel N. Baker[4], Robert E. Gold[1], Brian J. Anderson[1], Haje Korth[1], David Schriver[5], Ralph L. McNutt Jr.[1], and Sean C. Solomon[6,7]

[1]The Johns Hopkins University Applied Physics Laboratory, Laurel, Maryland, USA, [2]Physics Department, Catholic University of America, Washington, District of Columbia, USA, [3]Office of Space Research and Technology, Academy of Athens, Athens, Greece, [4]Laboratory for Atmospheric and Space Physics, University of Colorado, Boulder, Colorado, USA, [5]Department of Physics and Astronomy, University of California, Los Angeles, California, USA, [6]Department of Terrestrial Magnetism, Carnegie Institution of Washington, Washington, District of Columbia, USA, [7]Lamont-Doherty Earth Observatory, Columbia University, Palisades, New York, USA

Abstract The X-Ray Spectrometer (XRS) on the MErcury Surface, Space ENvironment, GEochemistry, and Ranging spacecraft regularly detected fluorescent X-rays near Mercury induced by low-energy (1–10 keV) or suprathermal electrons. We devised an algorithm to select these events from XRS records between April 2011 and March 2015 on the basis of their duration, location, and spectral slope. We identified 3102 events during 3900 orbits around Mercury, sampling all Mercury longitudes multiple times over the 4 year period. These suprathermal electrons were present near the planet at all local times, but the majority were on the nightside of the planet, and a dawn-dusk asymmetry is seen in the data. When the event locations are plotted in a coordinate system based on a simplified magnetic field model, several distinct clusters of events are evident. We infer that all are signatures of accelerated electrons that were injected from Mercury's tail region to form a quasi-trapped electron population at Mercury.

1. Introduction

The MErcury Surface, Space ENvironment, GEochemistry, and Ranging (MESSENGER) spacecraft entered orbit around Mercury on 18 March 2011. Upon exhausting all of its onboard propellant, MESSENGER impacted onto the planet on 30 April 2015. During its more than four Earth years of orbital operations, the spacecraft completed over 4000 orbits and made extensive measurements of the planet's surface, tenuous atmosphere, and highly dynamic magnetosphere. Prior to MESSENGER observations, little was known about the makeup of the energetic charged particle population in Mercury's magnetosphere. However, with the MESSENGER data, we now know that there are large populations of low-energy (~ keV) electrons in Mercury's magnetosphere [*Ho et al.*, 2011a]. From observations by the spacecraft's Energetic Particle and Plasma Spectrometer (EPPS) of electrons having energies between 35 keV and 1 MeV [*Andrews et al.*, 2007], *Ho et al.* [2011a] found that most of the intense moderate-energy (tens to hundreds of keV) electron events occurred on the nightside and at high northern latitudes. *Lawrence et al.* [2015] investigated the more energetic (>90 keV) electrons with data from the Neutron Spectrometer (NS) sensor, part of the MESSENGER Gamma-Ray and Neutron Spectrometer (GRNS) instrument [*Goldsten et al.*, 2007], and they found that these higher-energy electrons are located in a well-defined region at high latitudes, but equatorward of the boundary between open and closed field lines, in a quasi-permanent state. From EPPS measurements, *Ho et al.* [2011a] found that there was a set of events near the equator that had lower intensity and extended over most local times. *Ho et al.* [2011a] hypothesized that this group of low-energy, low-intensity events could be responsible for the electron-induced X-ray events that MESSENGER's X-Ray Spectrometer (XRS) [*Schlemm et al.*, 2007] measured during the spacecraft's Mercury flybys [*Ho et al.*, 2011b].

In this paper, we analyze the electron-induced X-ray events as measured by the XRS instrument on MESSENGER from April 2011, shortly after Mercury orbit insertion, to March 2015, less than 2 months before the end of spacecraft operations. These X-ray events have allowed us to characterize the distribution at Mercury of low-energy or suprathermal electrons, taken here as having energies from a few to a few tens of keV, just above the thermal energy range for solar wind electrons.

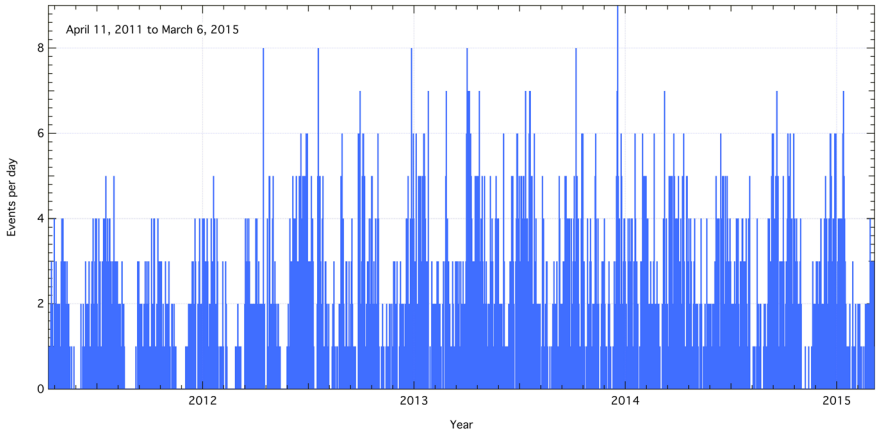

Figure 1. Rate of low-energy electron events as seen by the MESSENGER XRS from April 2011 to March 2015. There was an increase in the number of events per day in April 2012 because the spacecraft orbital period was changed from 12 h to 8 h. On average there were up to two events per orbit. There is also an ~88 day periodicity in the data because the MESSENGER orbital plane was fixed in the heliocentric inertial frame as Mercury orbited around the Sun every 88 days.

2. Observations

The MESSENGER XRS instrument had three nadir-pointing gas proportional counters (GPCs) that measured fluorescent X-rays (1–10 keV) from Mercury induced by solar X-rays incident onto its surface [*Schlemm et al.*, 2007]. Two of the GPCs were covered with thin Mg and Al foils to allow separation of the fluorescence lines of Mg and Al from that of Si at energies below ~2 keV. A Be-Cu collimator on the GPCs limited the field of view (FOV) to 12° full angle. *Ho et al.* [2011b] and *Starr et al.* [2012] modeled the XRS response to charged particles and found that self-fluorescent X-ray emission can also be generated within the collimator and entrance foils of the XRS GPCs from in situ low-energy (<10 keV) electrons. They found, in particular, that the self-fluorescent X-ray emission spectrum predicted from Mercury's electron distribution [*Ho et al.*, 2011b] was consistent with measured XRS spectra.

2.1. Selection Criteria

Since MESSENGER began orbital operations at Mercury in March 2011, XRS measured self-fluorescent X-rays generated by low-energy electrons inside Mercury's magnetosphere near periapsis on nearly every orbit. To catalogue these events systematically, we devised an automated algorithm to select fluorescence events on the basis of the following criteria: (1) the event must be less than 2 R_M from Mercury's center, where R_M is Mercury's radius (2440 km); (2) the duration of the event must be between 1 and 60 min; and (3) the ratio of the flux of the Mg line to that of the Al line from the foil-covered GPCs must be greater than unity.

The rationale for these criteria is as follows. As shown by *Lawrence et al.* [2015], energetic electron events are located in well-defined regions, close to the planet, and criterion 1 was selected on the basis of their results. All orbital space might have been interrogated by the search algorithm, but this criterion sped the search process considerably. Electron events interacting in the XRS detector material tended to be short-lived. By comparison, solar particle events may extend over many hours or even days. Criterion 2 was therefore included to eliminate solar particle events. Finally, both electron events and solar-flare-induced fluorescence from Mercury's surface enhanced the count rates in the Mg and Al lines detected by the XRS GPCs. However, the electron-induced enhancement of these lines was due to interaction with the XRS GPC filter material and differed in character from fluorescence from the planet. Criterion 3 excludes events from planetary fluorescence. In addition, we utilized the safing flag from the instrument to filter out those events generated by large solar particle events that triggered an instrument safe mode and rendered its response unreliable.

With these criteria we identified 3102 suprathermal electron events that occurred between 10 April 2011 and 6 March 2015. Figure 1 shows the number of events detected per day. On average, we measured two events during each orbit, typically just before and after each periapsis pass. During the first year of orbital operation, MESSENGER was in a 12 h orbit about Mercury with a maximum altitude of 15,000 km and a periapsis that varied between 200 and 500 km. MESSENGER's orbital period was reduced to 8 h in April 2012 and the

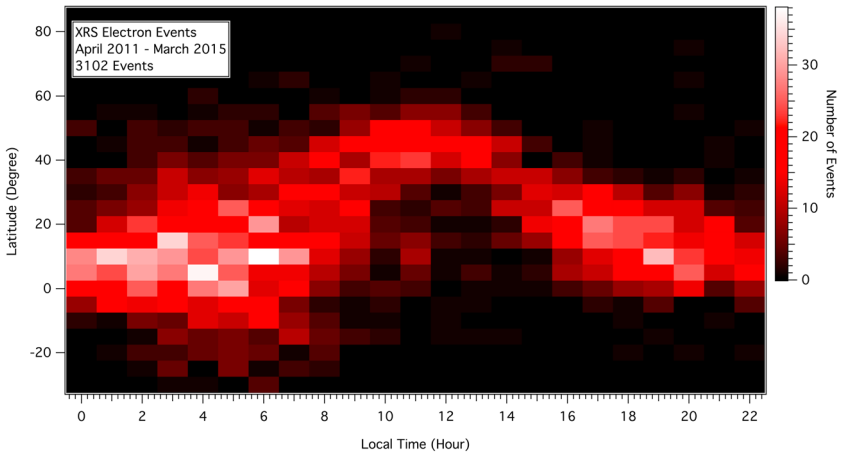

Figure 2. The distribution of suprathermal electron events by latitude and local time. The events spanned all local times but had the highest concentration in the dawn and dusk sectors. All events were clustered within a narrow band of latitudes, particularly around local noon.

apoapsis altitude to ~ 10,000 km in order to increase low-altitude coverage [*McAdams et al.*, 2014]. Hence, the maximum number of electron events detected per day increased from ~4 to ~6.

2.2. Event Locations

As shown in Figure 1, there is a periodicity in the frequency of suprathermal electron events at a period of 88 days, Mercury's orbital period. One interpretation of this periodicity is that there is a preferred local time for detecting these events, given that MESSENGER's orbital plane was fixed in the inertial frame and Mercury's orbit about the Sun is ~88 Earth days.

The locations of suprathermal electron events as a function of local time and geographic latitude are shown in Figure 2. Events were detected at all local times, but the highest concentrations were in the dawn and dusk sectors. Hence, a dawn-dusk orbit was most favorable for the observation of these electron events. *Ho et al.* [2011b] showed that suprathermal electrons have a very narrow pitch angle distribution, and the XRS with its 12° FOV further limited the pitch angle coverage. In terms of latitudinal distribution, the detected electron events were all clustered within a limited latitude band from −20° to 60°N. Events near local noon were most tightly clustered in latitudinal extent and at relatively high latitude (~40°–50°N), but events at other local times were also confined within bands that were centered north of the geographic equator by ~10°. We note that this latitudinal offset coincides approximately with the 484 km northward offset of Mercury's magnetic equator from the geographic equator [*Anderson et al.*, 2011]. MESSENGER's highly inclined (>82°) and eccentric orbit about Mercury prevented sampling of southernmost latitudes at low altitude, so we cannot tell if a band of suprathermal electron events is also present in the southern hemisphere.

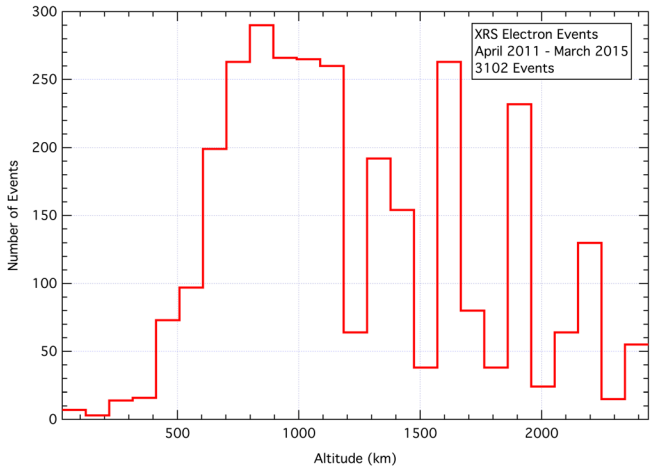

Figure 3. Histogram of spacecraft altitude at the time of detection of suprathermal electron events. Most events were at altitudes less than 1500 km, but there were several narrow bands at altitudes farther from the planet where electron events were common.

A comparison of the electron distribution between dawn and dusk indicates that there were twice as many events

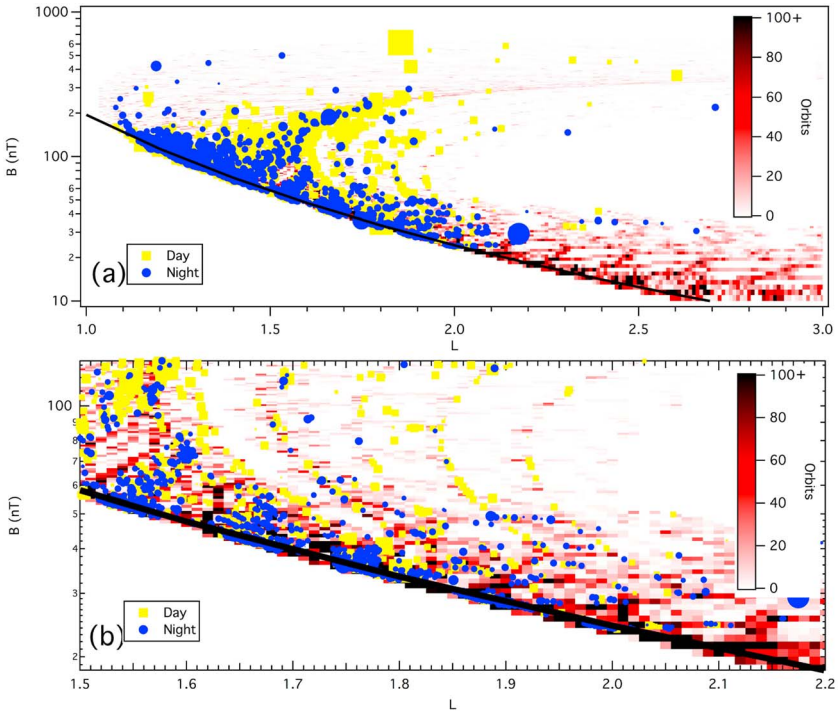

Figure 4. (a) Suprathermal electron events plotted in Mercury's *B* versus *L* coordinate system (see text). All 3102 events, both on the dayside (yellow squares) and nightside (blue circles), are shown. The size of the marker indicates the spectral index of the events, with larger symbols indicating harder spectra. The solid black line shows the magnetic equator. (b) A close-up of a portion of Figure 4a in the vicinity of the distinct bands of events at $L = 1.57$, 1.65, and 1.75. The color bar shows MESSENGER coverage during the time interval of our analysis.

in the dawn sector (~0500 h) as in the dusk (~1900 h) sector. In addition, the latitudinal spread was much wider in the dawn sector (~40°) than in the dusk sector (~20°). No events were detected north of 60°N. Figure 3 shows a histogram of the altitude of the MESSENGER spacecraft at the time of event detection. The majority of the events were at less than 1500 km altitude, and there were only nine events below 200 km, when MESSENGER was in its low-altitude campaign for the several months before the end of the mission. Above 1000 km altitude, there are bands at 1300 km, 1600 km, 1900 km, and 2200 km altitude within which there are clusters of events. We discuss these bands further below.

2.3. Magnetic Dipole Coordinates

Charged particle motion in a dipolar magnetosphere is best characterized in *McIlwain*'s [1961] *B*, *L* coordinate system, where *B* is the magnitude of the magnetic field vector and *L* is the distance (in planetary radii) at which a field line from the internal dipole crosses the magnetic equator. Following *Ho et al*. [2011a], we describe Mercury's internal field as a simple offset dipole:

$$B = \frac{M}{R^3}\sqrt{1 + 3\left(\frac{Z_M}{R}\right)^2}$$

$$L = \frac{R}{\sqrt{1 - \left(\frac{Z_M}{R}\right)^2}},$$

where $R = \sqrt{X^2 + Y^2 + Z_M^2}$ is the radial distance from the location of the magnetic dipole, the dipole moment M is 195 nT-$R_M{}^2$, $Z_M = Z - Z_0$ is the northward component of the radius vector from the dipole location, and $Z_0 = 484$ km.

The electron events show distinct localization when plotted in the *B*-*L* coordinate system, as seen in Figure 4a. Events on the dayside and nightside are distinguished in the figure, and the size of the marker denotes the measured ratio of Cu line flux (~9 keV) to that of the Mg and Al line fluxes (~1.5 keV) in the filtered GPCs, an

indicator of the electron spectral index. A larger symbol indicates that there were more electrons at higher energy (i.e., a harder spectrum), whereas smaller symbols denote softer spectra. The measured ratio of Cu line flux to Mg-Al line flux ranged from 0.1 to 2.0, with a mean of ~1.0. Figure 4b shows a close-up view from $L = 1.5$ to 2.2; at least three clusters of events ($L = 1.57$, 1.65, and 1.75) are seen to correspond to those displayed in Figure 3.

The population density of events in the *B*, *L* plot reflects both orbital coverage and event occurrence rate and spans a wide range of magnetic latitude and longitude [*McIlwain*, 1961]. The apparent curved structures, most prominent in the close-up in Figure 4b, are a consequence of orbital coverage systematics. The relative absence of events far from the magnetic equator (Figure 4) is in part the result of relatively sparse sampling in this region of *B*, *L* space, as suggested by the orbital coverage color bar. Nonetheless, the observation that the majority of the electron events were near the magnetic equator, at *L* values $< \sim 1.85$, particularly on the nightside, appears to be a real effect likely related to magnetotail acceleration processes. Moreover, the relative absence of events at $L > 2$ despite good orbital coverage is evidence that the dynamical phenomena depicted do not extend to the more distant magnetotail. On the dayside, there were many events apparently farther from the magnetic equator at larger values of *L*, as one might expect from the distortion of the dipolar field on Mercury's dayside by solar wind pressure.

3. Discussion and Summary

MESSENGER data show that energetic electrons at Mercury are abundant from the lowest energies (<10 keV) to energies of hundreds of keV [*Ho et al*., 2011b, 2012; *Lawrence et al*., 2015]. *Baker et al.* [2016] investigated the most intense energetic electron events as measured by MESSENGER's GRNS and found signatures of accelerated electrons being injected from the near-tail region and forming quasi-trapped populations. *Gershman et al*. [2015] also observed that during solar energetic particle events there are enhanced electron fluxes within the central plasma sheet that are indicative of an apparent trapped electron population at low latitudes in the magnetotail. *Ho et al*. [2012] speculated, on the basis of an earlier statistical study of higher-energy (>35 keV) electrons measured with the EPPS, that there are clusters of weaker events near the geographic equator. *Schriver et al*. [2011] showed with kinetic simulations that low-energy (1–10 keV) electrons can be quasi-trapped near Mercury's magnetic equator.

With the self-fluorescence measurements from the XRS, we have shown that there is a transient electron population around the magnetic equatorial region (Figures 2 and 4) at energies of a few keV, but with activity that also extends to higher latitudes, especially closer to the planet and on the dayside. Previous studies at higher energies [*Ho et al*., 2011a, 2011b, 2012; *Lawrence et al*., 2015; *Baker et al*., 2016] have shown that the energy range of this population extends from a few to several hundred keV. These electrons are predominantly in the dawn sector, at a frequency approximately twice that of the dusk sector, consistent with electron drift in the direction from midnight toward dawn around the planet due to ∇B and radius and curvature drift. There is a wider latitudinal spread (~20–40°) of these electron events, with the widest spread in the dawn sector. At local noon, the latitudinal extent of the detected events is shifted northward by ~30°, a shift that follows closely the boundary between open and closed field lines, as shown by *Korth et al*. [2014] and *Lawrence et al*. [2015].

These electron events in most cases were seen shortly before or after spacecraft periapsis at low altitude (<1500 km). When plotted in the *B*-*L* coordinate system, most of the nightside events were in the near-equatorial region (Figure 4a), and some of the dayside events were at higher altitudes farther from the planet. Most of the events in the near-equatorial region had a moderate spectral index (Cu/Mg-Al ~1.0) compared with those at higher latitude. On the dayside, events with the hardest spectra (Cu/Mg-Al ~ 1.5–2.0) were at higher latitudes. This last group of events was close to the boundary between open and closed magnetic field lines.

The XRS data show that there are distinct bands within which suprathermal electrons cluster in Mercury's magnetosphere. These observations suggest that the electrons could drift in longitude along closed field lines, as demonstrated in a few cases at higher energies by echoes [*Baker et al*., 2016], and that there could be quasi-trapped electrons in orbits close to Mercury's magnetic equator as a more or less standard feature. We refer to these particles as quasi-trapped because most of the electrons at these energies (~ keV) cannot completely drift around the planet before either striking the surface or hitting the dayside magnetopause, and only a few make a complete orbit around the planet [*Schriver et al*., 2011; *Starr et al*., 2012]. However,

the fact that we detected these electrons on almost every orbit indicates that they represent a semipermanent feature. *Baker et al*. [1986] and *Birn et al*. [2012] proposed that inductive electric fields associated with reconnection are sufficient to accelerate electrons up to hundreds of keV on very short time scales. *Slavin et al*. [2009, 2010] showed that the reconnection rate at Mercury is a factor of 10 greater than at Earth and documented large flux transfer events at the magnetosheath and multiple traveling compression regions in the magnetotail. Accelerated electrons at high energies measured by *Lawrence et al*. [2015] with GRNS could not completely drift around the planet before being lost [*Schriver et al*., 2011]. But at the energies of electrons measured by XRS, and at all longitudes, it is possible that some could still drift to the dusk side without being lost. The high-latitude events observed at local noon, however, had harder energy spectra and were close to the boundary between open and closed field lines as identified by *Korth et al*. [2014] and *Lawrence et al*. [2015].

In summary, 4 years of MESSENGER XRS observations from orbit about Mercury show that suprathermal electrons in the energy range from a few keV to a few tens of keV are typically present, particularly close to the planet's magnetic equator. The majority of the events are on the nightside of the planet, and a dawn-dusk asymmetry is seen in the data. These properties are not substantially different from those reported at higher energies, up to hundreds of keV, suggesting that the events analyzed here constitute the lower-energy end of a population common to all energetic electron events at Mercury. By inference, the events documented here may well have an origin similar to that of the higher-energy electron events. All these observations support the hypothesis that electrons are being accelerated in Mercury's tail region through reconnection and/or dipolarization events and then drift around the planet to form a quasi-permanent population.

Acknowledgments
The MESSENGER mission is supported by the NASA Discovery Program under contracts NAS5-97271 to The Johns Hopkins University Applied Physics Laboratory and NASW-00002 to the Carnegie Institution of Washington. All MESSENGER data analyzed for this paper are publicly available at the NASA Planetary Data System.

References

Anderson, B. J., C. L. Johnson, H. Korth, M. E. Purucker, R. M. Winslow, J. A. Slavin, S. C. Solomon, R. L. McNutt Jr., J. M. Raines, and T. H. Zurbuchen (2011), The global magnetic field of Mercury from MESSENGER orbital observations, *Science*, *333*, 1859–1862, doi:10.1126/science.1211001.

Andrews, G. B., et al. (2007), The Energetic Particle and Plasma Spectrometer instrument on the MESSENGER spacecraft, *Space Sci. Rev.*, *131*, 523–556.

Baker, D. N., J. A. Simpson, and J. H. Eraker (1986), A model of impulsive acceleration and transport of energetic particles in Mercury's magnetosphere, *J. Geophys. Res.*, *91*, 8742–8748, doi:10.1029/JA091iA08p08742.

Baker, D. N., et al. (2016), Intense energetic-electron flux enhancements in Mercury's magnetosphere: An integrated view with high-resolution observations from MESSENGER, *J. Geophys. Res. Space Physics*, doi:10.1002/2015JA021778, in press.

Birn, J., A. V. Artemyev, D. N. Baker, M. Echim, M. Hoshino, and L. M. Zelenyi (2012), Particle acceleration in the magnetotail and aurora, *Space Sci. Rev.*, *173*, 49–102, doi:10.1007/s11214-012-9874-4.

Gershman, D. J., et al. (2015), MESSENGER observations of solar energetic electrons within Mercury's magnetosphere, *J. Geophys. Res. Space Physics*, *120*, 8559–8571, doi:10.1002/2015JA021610.

Goldsten, J. O., et al. (2007), The MESSENGER Gamma-Ray and Neutron Spectrometer, *Space Sci. Rev.*, *131*, 339–391, doi:10.1007/s11214-007-9262-7.

Ho, G. C., et al. (2011a), MESSENGER observations of transient bursts of energetic electrons in Mercury's magnetosphere, *Science*, *333*, 1865–1868, doi:10.1126/science.1211141.

Ho, G. C., R. D. Starr, R. E. Gold, S. M. Krimigis, J. A. Slavin, D. N. Baker, B. J. Anderson, R. L. McNutt Jr., L. R. Nittler, and S. C. Solomon (2011b), Observations of suprathermal electrons in Mercury's magnetosphere during the three MESSENGER flybys, *Planet. Space Sci.*, *59*, 2016–2025.

Ho, G. C., S. M. Krimigis, R. E. Gold, D. N. Baker, B. J. Anderson, H. Korth, J. A. Slavin, R. L. McNutt Jr., R. M. Winslow, and S. C. Solomon (2012), Spatial distribution and spectral characteristics of energetic electrons in Mercury's magnetosphere, *J. Geophys. Res.*, *117*, A00M04, doi:10.1029/2012JA017983.

Korth, H., B. J. Anderson, D. J. Gershman, J. M. Raines, J. A. Slavin, T. H. Zurbuchen, S. C. Solomon, and R. L. McNutt Jr. (2014), Plasma distribution in Mercury's magnetosphere derived from MESSENGER Magnetometer and Fast Imaging Plasma Spectrometer observations, *J. Geophys. Res. Space Physics*, *119*, 2917–2932, doi:10.1002/2013JA019567.

Lawrence, D. J., et al. (2015), Comprehensive survey of energetic electron events in Mercury's magnetosphere with data from the MESSENGER Gamma-Ray and Neutron Spectrometer, *J. Geophys. Res. Space Physics*, *120*, 2851–2876, doi:10.1002/2014JA020792.

McAdams, J. V., C. G. Bryan, D. P. Moessner, B. R. Page, D. R. Stanbridge, and K. E. Williams (2014), Orbit design and navigation through the end of MESSENGER's extended mission at Mercury, 24th Space Flight Mechanics Meeting, American Astronautical Society/American Institute of Aeronautics and Astronautics, paper AAS 14-369, 20 pp., Santa Fe, New Mex., 26–30 Jan.

McIlwain, C. E. (1961), Coordinates for mapping the distribution of magnetically trapped particles, *J. Geophys. Res.*, *66*, 3681–3691, doi:10.1029/JZ066i011p03681.

Schlemm, C. E., II, et al. (2007), The X-Ray Spectrometer on the MESSENGER spacecraft, *Space Sci. Rev.*, *131*, 393–415.

Schriver, D., et al. (2011), Quasi-trapped ion and electron populations at Mercury, *Geophys. Res. Lett.*, *38*, L23103, doi:10.1029/2011GL049629.

Slavin, J. A., et al. (2009), MESSENGER observations of magnetic reconnection in Mercury's magnetosphere, *Science*, *324*, 606–610, doi:10.1126/science.1172011.

Slavin, J. A., et al. (2010), MESSENGER observations of extreme loading and unloading of Mercury's magnetic tail, *Science*, *329*, 665–668, doi:10.1126/science.1188067.

Starr, R. D., D. Schriver, L. R. Nittler, S. Z. Weider, P. K. Byrne, G. C. Ho, E. A. Rhodes, C. E. Schlemm II, S. C. Solomon, and P. Trávníček (2012), MESSENGER detection of electron-induced X-ray fluorescence from Mercury's surface, *J. Geophys. Res.*, *117*, E00L02, doi:10.1029/2012JE004118.